



Alterations in metabolic pathways in stomach of mice infected with *Helicobacter pylori*

Nishiumi, Shin
Yoshida, Masaru
Azuma, Takeshi

(Citation)

Microbial Pathogenesis, 109:78-85

(Issue Date)

2017-08

(Resource Type)

journal article

(Version)

Accepted Manuscript

(Rights)

© 2017 Elsevier B.V.

This manuscript version is made available under the CC-BY-NC-ND 4.0 license
<http://creativecommons.org/licenses/by-nc-nd/4.0/>

(URL)

<https://hdl.handle.net/20.500.14094/90006179>



Manuscript Details

Manuscript number	YMPAT_2017_188
Title	Alterations in metabolic pathways in stomach of mice infected with <i>Helicobacter pylori</i>
Article type	Research Paper

Abstract

Numerous studies of *Helicobacter pylori* (*H. pylori*) have been performed, but few studies have evaluated the effects of *H. pylori* infections using metabolome analysis, which involves the comprehensive study of low molecular weight metabolites. In this study, the metabolites in the stomach tissue of mice that had been infected with *H. pylori* SS1 for 1, 3, or 6 months were analyzed, and then evaluations of various metabolic pathways were performed to gain novel understandings of *H. pylori* infections. As a result, it was found that the glycolytic pathway, the tricarboxylic acid cycle, and the choline pathway tended to be upregulated at 1 month after the *H. pylori* SS1 infection. The urea cycle tended to be downregulated at 6 months after the infection. High levels of some amino acids were observed in the stomach tissue of the *H. pylori* SS1-infected mice at 1 month after the infection, whereas low levels of many amino acids were detected at 3 and 6 months after the infection. These results suggest that *H. pylori* infection causes various metabolic alterations at lesion sites, and these alterations might be linked to the crosstalk between *H. pylori* and the host leading to transition of disease conditions.

Keywords	<i>Helicobacter pylori</i> ; Metabolome analysis; Liquid chromatography/mass spectrometry; Gas chromatography/mass spectrometry; Metabolite
Corresponding Author	Shin Nishiumi
Order of Authors	Shin Nishiumi, Masaru Yoshida, Takeshi Azuma
Suggested reviewers	Sumio Ohtsuki, Takeshi Bamba, Fumio Matsuda

Submission Files Included in this PDF

File Name [File Type]

Cover_letter(Nishiumi et al)_final.docx [Cover Letter]

Response_to_Editor_and_Reviewers_final.docx [Response to reviewers]

Manuacript (Nishiumi et al)_final.docx [Manuscript]

Figure (Nishiumi et al).pptx [Figure]

Table (Nishiumi et al).docx [Table]

Supplemental Figure (Nishiumi et al).pdf [e-Component]

Highlight (Nishiumi et al)final.docx [Highlights]

To view all the submission files, including those not included in the PDF, click on the manuscript title on your EVISE Homepage, then click 'Download zip file'.

Division of Gastroenterology,
Department of Internal Medicine,
Kobe University Graduate School of Medicine,
7-5-1 Kusunoki-cho, Chu-o-ku,
Kobe, Hyogo 650-0017, Japan.
Tel: +81-78-382-6305 FAX: +81-78-382-6309
E-mail: nishiums@med.kobe-u.ac.jp
May 15, 2017

Editor-in-Chief:
Microbial Pathogenesis
Dear Dr Gorvel,

Thank you for your e-mail of May 15, 2017 regarding our manuscript entitled “Alterations in metabolic pathways in stomach of mice infected with *Helicobacter pylori*” (The title was modified via the first revision of our manuscript) by Shin Nishiumi, Masaru Yoshida, Takeshi Azuma (YMPAT_2017_188_R1). We attach here our revised manuscript as well as point-by-point responses to the Editor’s and Reviewers’ comments. All authors contribute to this research and are in agreement with its publication in *Microbial Pathogenesis*. Moreover, none of the work described in this paper has been published elsewhere, and all authors declare that they have no conflict of interest.

We consider that the revised manuscript includes the suitable response to Editor’s and Reviewers’ comments, and moreover has been improved over the initial submission. We trust that it is suitable for publication in *Microbial Pathogenesis*.

Thank you in advance for your kind consideration of this manuscript.

Sincerely yours,

Shin Nishiumi

Response to Editor and Reviewers

Dear Editor and Reviewers,

Thank you very much for your constructive and helpful comments to improve the impact of our manuscript (YMPAT_2017_188_R1). According to your comments and suggestions, we have modified our manuscript as described below. The revised parts have been highlighted in green (The yellow-highlighted letters show the parts modified in the first revision).

Comments from the editors and reviewers:

-Reviewer 1

- Most of the criticisms have been solve in the revised manuscript.

Please just consider to mention "The existence of H. pylori in stomach was confirmed by PCR." in the materials and methods.

Response: Thank you for your comment. According to your suggestion, we added the ‘The existence of H. pylori SS1 in the stomach tissue was confirmed by PCR.’ in the Materials and Methods section (page 5, line 102).

-Reviewer 2

- The current version of the manuscript should be accepted without additional revision,

Response: Thank you very much for reviewing our manuscript.

1 **Alterations in metabolic pathways in stomach of mice infected with *Helicobacter pylori***

2

3 Shin Nishiumi^{a,*}, Masaru Yoshida^{a,b,c}, Takeshi Azuma^a

4

5 ^aDivision of Gastroenterology, Department of Internal Medicine, Kobe University Graduate School
6 of Medicine, 7-5-1 Kusunoki-cho, Chuo-ku, Kobe, Hyogo 650-0017, Japan

7 ^bDivision of Metabolomics Research, Department of Internal Related, Kobe University Graduate
8 School of Medicine, 7-5-1 Kusunoki-cho, Chuo-ku, Kobe, Hyogo 650-0017, Japan

9 ^cAMED-CREST, AMED, 7-5-1 Kusunoki-cho, Chuo-ku, Kobe, Hyogo 650-0017, Japan

10

11 *Corresponding author: Shin Nishiumi

12 Division of Gastroenterology, Department of Internal Medicine, Kobe University Graduate School
13 of Medicine, 7-5-1 Kusunoki-cho, Chuo-ku, Kobe, Hyogo 650-0017, Japan

14 E-mail: nishiums@med.kobe-u.ac.jp

15 TEL: +81-78-382-6305

16 FAX: +81-78-382-6309

17

18 **Abstract**

19 Numerous studies of *Helicobacter pylori* (*H. pylori*) have been performed, but few studies
20 have evaluated the effects of *H. pylori* infections using metabolome analysis, which involves the
21 comprehensive study of low molecular weight metabolites. In this study, the metabolites in the
22 stomach tissue of mice that had been infected with *H. pylori* SS1 for 1, 3, or 6 months were analyzed,
23 and then evaluations of various metabolic pathways were performed to gain novel understandings of
24 *H. pylori* infections. As a result, it was found that the glycolytic pathway, the tricarboxylic acid cycle,
25 and the choline pathway tended to be upregulated at 1 month after the *H. pylori* SS1 infection. The
26 urea cycle tended to be downregulated at 6 months after the infection. High levels of some amino
27 acids were observed in the stomach tissue of the *H. pylori* SS1-infected mice at 1 month after the
28 infection, whereas low levels of many amino acids were detected at 3 and 6 months after the
29 infection. These results suggest that *H. pylori* infection causes various metabolic alterations at
30 lesional sites, and these alterations might be linked to the crosstalk between *H. pylori* and the host
31 leading to transition of disease conditions.

32

33

34 **Keywords**

35 *Helicobacter pylori*; Metabolome analysis; Liquid chromatography/mass spectrometry; Gas
36 chromatography/mass spectrometry; Metabolite

37

38 **Abbreviations**

39 *H. pylori*, *Helicobacter pylori*; MALT, mucosa-associated lymphoid tissue; LC/MS, liquid
40 chromatography/mass spectrometry; GC/MS, gas chromatography/mass spectrometry; TCA,
41 tricarboxylic acid; IDO, indoleamine 2,3-dioxygenase.

42

43 **1. Introduction**

44 Helicobacter pylori (*H. pylori*) is a Gram-negative microaerophilic bacterium that
45 chronically colonizes the gastric epithelium of more than 50% of the world's population. This
46 bacterium plays an important role in the development of several gastrointestinal diseases including
47 non-symptomatic chronic gastritis, peptic ulcer disease, gastric mucosa-associated lymphoid tissue
48 (MALT) lymphoma, and gastric adenocarcinoma [1-3]. Furthermore, it has been categorized as a
49 group I carcinogen in humans [4]. The outcomes of such diseases depend on multiple factors like
50 host immune gene polymorphisms and the amount of gastric acid present in the stomach. *H. pylori*
51 virulence factors, such as the cytotoxin-associated gene pathogenicity island-encoded protein CagA
52 and the vacuolating cytotoxin VacA, are also important, e.g., these cytotoxins appear to modulate the
53 host's immune system [5].

54 In this study, we explored the pathogenesis of *H. pylori* infections using
55 metabolomics/metabolome analysis. Metabolomics/metabolome analysis involves the
56 comprehensive study of low molecular weight metabolites; i.e., the levels of such metabolites are
57 assessed in order to determine the cellular processes that occur in a particular cell type, tissue, organ,
58 or organism. The metabolome represents the endpoint of the omics cascade so it is also the closest
59 point in the cascade to the phenotype. The genome, which is found in the upstream part of the omics
60 cascade and contains numerous genes, is basically not affected by exogenous factors, such as
61 environmental and dietary factors. Even if a certain gene contains a mutation, the host's body might
62 remain unchanged due to the effects of homeostatic processes. In addition to variations in DNA,
63 mRNA, and protein expression, the metabolome is also affected by the enzymatic activities of
64 various proteins, and alterations in the levels of metabolites can also be caused by exogenous factors;
65 therefore, the metabolomic profiles can be located in a summary of the other upstream omics profiles.
66 Thus, the metabolome analysis might be able to express subtle alterations in metabolic pathways and
67 deviations from homeostasis before phenotypic changes arise [6,7], and hence, could be useful for *H.*
68 *pylori*-related researches.

69 In this study, C57BL/6J mice were orally infected with *H. pylori* SS1, a mouse-adapted
70 strain, and their stomach tissue was collected at 1, 3, or 6 months after the infection. The metabolites

71 in the stomach tissues were analyzed using liquid chromatography/mass spectrometry (LC/MS) and
72 gas chromatography/mass spectrometry (GC/MS). Evaluations based on the glycolytic pathway,
73 tricarboxylic acid (TCA) cycle, choline pathway, urea cycle, glutathione cycle, purine pathway,
74 pyrimidine pathway, and amino acid metabolism were also performed via the metabolite profiling.
75

76 **2. Materials and Methods**

77 *2.1. Helicobacter pylori culture*

78 The *H. pylori* SS1 strain, which was originally collected from the patient with peptic ulcer
79 disease and is available for infecting mice, was used in this study. *H. pylori* SS1 was cultured on
80 Columbia agar plates (Becton, Dickinson and Company, Tokyo, Japan) under microaerobic
81 conditions (5% O₂, 5% CO₂, and 90% N₂) at 37°C. One colony was picked from each culture plate,
82 inoculated on a new agar plate, and cultured under the same conditions. Before the animal
83 experiments, *H. pylori* SS1 were grown in Brucella broth supplemented with 10% fetal bovine serum
84 overnight.

85

86 *2.2. Animal experiments*

87 All of the animal experiments performed in this study were approved by the Institutional
88 Animal Care and Use Committee and carried out according to the Kobe University Animal
89 Experimentation Regulations. C57BL/6J mice were purchased from CLEA Japan (Tokyo, Japan).
90 All mice were housed and bred at the animal unit of the Kobe University School of Medicine in a
91 specific pathogen-free facility under an approved experimental protocol. C57BL/6J mice (female, 5-
92 weeks-old, N=12) were orally infected with *H. pylori* SS1 (2 x 10⁸ CFU per an injection). As a
93 negative control, C57BL/6J mice (female, 5-weeks-old, N=12) were orally injected with PBS alone.
94 In this study, the *H. pylori* SS1 infection was performed by its single injection. One, 3, and 6 months
95 after the infection procedure, the mice were sacrificed, and then their stomach tissue was collected.
96 All mice for 1, 3 and 6 month *H. pylori* SS1 infection were subjected to its orally single
97 injection at the same time. In this study, 12 of C57BL/6J mice orally infected with *H. pylori*
98 SS1, and then each the 4 mice infected with *H. pylori* SS1 were sacrificed at each the period of
99 1, 3, or 6 months. In addition, as a negative control, 12 of C57BL/6J mice were orally injected
100 with PBS alone, and each the 4 mice were sacrificed as the corresponding control mice for each
101 the infection period. Therefore, the number of infection groups and the corresponding non-
102 infection groups was N=4 each. The existence of *H. pylori* SS1 in the stomach tissue was confirmed
103 by PCR. The collected stomach tissue samples were subjected to hematoxylin and eosin (HE)

104 staining for pathological evaluation, and LC/MS and GC/MS analyses to obtain metabolite
105 measurements.

106

107 *2.3. HE staining*

108 The stomach tissue samples collected from the mice were dissected and fixed with 10%
109 formalin, and then the paraffin-embedded tissue was sliced at 5 μm and stained with HE in a blinded
110 manner. The resultant sections were examined using a microscope (BX51; OLYMPUS, Tokyo,
111 Japan).

112

113 *2.4. LC/MS analysis*

114 During the LC/MS-based measurement of anionic and cationic metabolites, metabolites
115 were extracted from the stomach tissue samples according to the methods described in our previous
116 report [8]. The resultant solution containing the extracted metabolites was subjected to LC/MS
117 analysis. The LC/MS measurements were carried out using a Nexera LC system (Shimadzu Corp.,
118 Kyoto, Japan) equipped with two LC-30AD pumps, a DGU-20A5 degasser, an SIL-30AC
119 autosampler, a CTO-20AC column oven, and a CBM-20A control module, coupled to an LCMS-
120 8040 triple quadrupole mass spectrometer (Shimadzu Corp.). The data analysis for the semi-
121 quantitative evaluation was performed in accordance with the previously described method [8,9].

122

123 *2.5. GC/MS analysis*

124 During the GC/MS analysis, metabolites were extracted from the stomach tissue samples
125 in accordance with the methods described in our previous report [10]. The GC/MS measurements
126 were carried out using a GCMS-QP2010 Ultra (Shimadzu, Kyoto, Japan) with a fused silica
127 capillary column (CP-SIL 8 CB low bleed/MS; inner diameter: 30 μm \times 0.25 mm, film thickness:
128 0.25 μm ; Agilent Co., Palo Alto, CA). The data analysis for the semi-quantitative evaluation was
129 performed in accordance with the method described in our previous report [10].

130

131 *2.6. Statistical analysis*

132 The F-test was used to compare the variances of each group, and then the Student's t-test
133 was employed to evaluate the significance of the differences between each group. The P-values of
134 less than 0.05 were judged to indicate a significant difference. Principal component analysis was
135 performed using the JMP9 software (SAS Institute Inc., Cary, NC), and the score plots for the first
136 three components were evaluated.
137

138 **3. Results**

139 In this study, C57BL/6J mice were infected with *H. pylori* SS1, which is a mouse-adapted
140 *H. pylori* strain. *H. pylori* SS1 is a cagA-positive and vacA s2/m2-positive strain and is used to
141 produce mouse infection models. First, the pathological appearance of the stomach tissues of the
142 mice was confirmed at 1, 3, and 6 months after the *H. pylori* SS1 infection (**Figure 1**). As a result, it
143 was found that *H. pylori* SS1 infection causes the development of abnormal gastric mucosa
144 architecture. Inflammatory cell invasion was also detected throughout the observation period. Six
145 months after the infection, foveolar hyperplasia was observed, and the gastric pits and glands were
146 longer than those of uninfected age-matched mice.

147 Next, using LC/MS we analyzed the metabolites in the stomach tissue samples collected
148 from the mice at 1, 3, and 6 months after the *H. pylori* SS1 infection and the corresponding control
149 mice. Then, evaluations based on particular metabolic pathways, including the glycolytic pathway,
150 TCA cycle, choline pathway, urea cycle, glutathione cycle, purine pathway, pyrimidine pathway,
151 and amino acid metabolism, were carried out (**Table 1, Supplemental Figure 1**). GC/MS analysis
152 was used to detect metabolites related to these pathways that were not detected by LC/MS, and the
153 results of this analysis were added into the pathway-based evaluations (**Table 1, Supplemental**
154 **Figure 1**). The levels of metabolites existed in the glycolytic pathway tended to be upregulated in
155 the mice that had been infected with *H. pylori* SS1 for 1 month, but no such tendency was observed
156 at 3 or 6 months after the *H. pylori* SS1 infection. The levels of metabolites linked to the TCA cycle
157 tended to be upregulated at 1 month after the *H. pylori* SS1 infection. Regarding the levels of
158 metabolites related to the choline pathway, they were increased at 1 month after the *H. pylori* SS1
159 infection. As for the purine and pyrimidine pathways, the production of uracil was increased at 6
160 months after the *H. pylori* SS1 infection. The levels of metabolites related to the urea cycle tended to
161 be reduced at 6 months after the *H. pylori* SS1 infection. It was difficult to judge the alterations
162 induced in the glutathione pathway by *H. pylori* SS1 infection. As for amino acid metabolism, **the**
163 **tendency in the high levels of some amino acids, such as alanine + sarcosine, glutamine, and**
164 **glutamate, of which the fold induction values were more than 1.2 compared with the corresponding**
165 **control mice, were observed in the stomach tissues of the *H. pylori* SS1-infected mice at 1 month**

166 after the infection, but low levels of many amino acids, such as arginine, asparagine, histidine,
167 phenylalanine, tyrosine, γ -aminobutyrate (GABA), of which the fold induction values were
168 significantly decreased compared with the corresponding control mice, were detected at 3 and 6
169 months after the infection.

170 The same evaluations were performed for other metabolites; i.e., metabolites that were not
171 related to the glycolytic pathway; TCA cycle; choline pathway; urea cycle; glutathione cycle; purine
172 pathway; pyrimidine pathway; or amino acid metabolism, including the glutamine pathway and
173 tryptophan cycle (**Table 2**). The levels of glycerate and serotonin in the stomach tissues of the *H.*
174 *pylori* SS1-infected mice were significantly changed at 1 month after the infection. At 3 months after
175 the infection, the level of 2-hydroxy-glutarate was significantly decreased, and significant alterations
176 in the levels of 3-hydroxy-butyrate, 2-hydroxy-3-methyl-butyrate, carnosine, N-acetylglycine, L-
177 pyroglutamate, and uric acid were observed at 6 months after the infection.

178 Finally, the principal component analysis based on the metabolite profiles was carried out
179 to understand the similarities of metabolite profile among groups (**Figure 2**). As a result, there were
180 no distinct differences in the metabolite profiles on the score plots for the first three components,
181 indicating that metabolite alterations may be independent on the infection periods.

182

183 **4. Discussion**

184 *H. pylori* infections are known to cause a variety of gastrointestinal diseases, such as non-
185 symptomatic chronic gastritis, peptic ulcer disease, gastric adenocarcinoma, and gastric MALT
186 lymphoma [1-3], and the related molecular mechanisms underlying these diseases are beginning to
187 be elucidated in studies of both the host and bacteria. However, few studies have evaluated the host
188 alterations induced by *H. pylori* infection using metabolome analysis (to the best of our knowledge
189 only one such study has been published) [11]. In the latter study [11], urine was collected from
190 gerbils that had been infected with *H. pylori* (a clinical isolate that is known to undergo long-term
191 adaptation in gerbils), and the metabolites in the urine were analyzed using proton nuclear magnetic
192 resonance spectrometry. From these results, it was suggested that *H. pylori* infections disturb
193 carbohydrate metabolism and generate marked changes in amino acid metabolism. In addition, it
194 was shown that *H. pylori* infection changes the gut microbiota, as exhibited by changes in the
195 microbial-related metabolites. However, *H. pylori* infections affect the host's stomach, as do most of
196 the related diseases. In addition, alterations in urinary metabolite levels do not necessarily
197 correspond to the changes in metabolite levels that occur in the stomach tissues. Therefore, the
198 metabolomic analysis of stomach tissues collected from *H. pylori*-infected animals is a useful way of
199 obtaining novel findings regarding *H. pylori* infections.

200 Previously, transcriptome analysis, which involves the large-scale and comprehensive
201 study of mRNA, and the proteome analysis; i.e., the large-scale and exhaustive study of proteins,
202 were used to evaluate the effects of *H. pylori* infection on the host. For example, the mRNA and
203 protein profiles of AGS cells that had been infected with wild-type *H. pylori* or *cag* pathogenicity
204 island mutant strains of the bacterium were evaluated [12]. In the latter study, cDNA expression
205 array analysis of mRNA expression was used to target 6 functional groups, including (i) cell cycle
206 regulating genes, (ii) stress responsive and intracellular signaling-associated genes, (iii) apoptosis-
207 associated genes, (iv) DNA repair and recombination-associated genes, (v) transcription factors and
208 (vi) cell adhesion molecules connected to cell-cell communication, and the altered molecules
209 connected to transcriptional responses, the regulation of cell adhesion and actin cytoskeletal
210 rearrangement, and cell cycle modulation were observed. In addition, CagA-dependent changes were

211 detected during the analyses of the cells' mRNA and protein profiles. From gene profiling of human
212 gastric mucosa tissue that had been infected with *H. pylori* [13], 8 factors, GATA6, signal transducer
213 and activator of transcription 6 (STAT6), matrix metalloproteinase 7 (MMP7), chemokine (C-X-C
214 motif) ligand 13 (CXCL13), ubiquitin protein D, mitogen-activated protein kinase 8 (MAPK8),
215 lymphocyte antigen 96 (LY96), and whey acidic protein four-disulfide core domain protein 2
216 (WFDC2), were identified as risk factors for *H. pylori* infection. In a study by Nookaew et al. [14],
217 transcriptome analysis showed that in atrophic gastritis caused by *H. pylori* the defective expression
218 of genes associated with acid secretion, energy metabolism, and blood clotting contributes to
219 antralization of the corpus mucosa. In addition, corpus atrophication was also found to be associated
220 with the upregulation of genes connected to inflammation and cell signaling [14]. Thus, a number of
221 studies have evaluated *H. pylori* infections using the transcriptome and proteome analysis, but the
222 number of such studies is small, and furthermore, the conclusions of these studies were often
223 connected to inflammation, the cell cycle, or cell adhesion, and were mainly derived from molecular
224 biology or biochemical techniques. Our study evaluated several metabolic pathways including the
225 glycolytic pathway, TCA cycle, choline pathway, urea cycle, glutathione cycle, purine pathway,
226 pyrimidine pathway, and amino acid metabolism based on metabolite profiles, and *H. pylori*
227 infection-induced alterations were observed in some host metabolic pathways. Furthermore, we
228 found differences in these pathways between the early and late phases of the infection. For example,
229 the trends in high levels of some amino acids, such as alanine + sarcosine, glutamine, and glutamate,
230 of which the fold induction values were more than 1.2 compared with the corresponding control
231 mice, were observed in the stomach tissues of the *H. pylori* SS1-infected mice at 1 month after the
232 infection (the early phase), whereas low levels of many amino acids, such as arginine, asparagine,
233 histidine, phenylalanine, tyrosine, GABA, of which the fold induction values were significantly
234 decreased compared with the corresponding control mice, were seen in the stomach tissue of the *H.*
235 *pylori* SS1-infected mice at 3 and 6 months after the infection (the late phase). Some amino acids are
236 used for energy production in cells, and the reductions in the levels of these amino acids seen during
237 the late phase might have been due to excessive energy consumption along with increases in the
238 number of infiltrating immune cells. Also, amino acid levels and inflammation/immunity are often

239 related. For example, glutamine can ameliorate *H. pylori*-induced gastric inflammatory diseases *in*
240 *vivo* [15,16]. In addition, glutamine could reduce gastritis and epithelial hyperproliferation in gerbils
241 infected with *Helicobacter suis*, which belongs to the Helicobacter family just like *H. pylori* and is a
242 Gram-negative bacterium that colonizes in the stomachs of various animals [17]. In the current study,
243 an increased level of kynurenine was observed in the stomach tissues of the *H. pylori*-infected mice.
244 Kynurenine is produced from tryptophan by indoleamine 2,3-dioxygenase (IDO). It was previously
245 reported that IDO expression is enhanced by *H. pylori* infection [18,19], and IDO is strongly
246 expressed in immune cells. Therefore, the increased level of kynurenine seen in this study might
247 have been caused by infiltrating immune cells that had been attracted by the *H. pylori* infection. In
248 the stomach tissues of the mice that were infected with *H. pylori* SS1 for 6 months, the level of
249 carnosine was significantly decreased. Carnosine, which is a dipeptide molecule composed of β -
250 alanine and histidine, is a scavenger of reactive oxygen species and can reduce oxidative stress [20].
251 Therefore, a *H. pylori*-induced reduction in the level of carnosine might lead to the upregulation of
252 oxidative stress and the progression of *H. pylori*-related diseases. The level of GABA tended to be
253 decreased in the stomach tissues of the *H. pylori* SS1-infected mice at 1 and 3 months after the
254 infection, and was significantly reduced at 6 month. GABA mainly works as the inhibitory
255 neurotransmitter in brain, but has other functions in various tissues except brain. For example,
256 GABA could promote the proliferation of the gastric cancer cell line [21]. In the stomach of the mice
257 infected with *H. pylori*, the epithelial hyperproliferation is observed. Therefore, the *H. pylori* SS1-
258 caused decreased level of GABA may explain upregulation of GABA availability in *H. pylori* SS1-
259 induced epithelial hyperproliferation.

260 As shown above, metabolite profiles can lead to novel findings regarding *H. pylori*-
261 induced host biological responses, and our metabolome analysis-based study obtained meaningful
262 novel findings about *H. pylori* infections. However, during *H. pylori* infections various types of cells
263 infiltrate into the host's stomach tissues. For example, T cells and B cells are known to infiltrate into
264 such lesions, although the frequencies of each cell type differ among the various diseases caused by
265 *H. pylori* [22,23]. Therefore, to elucidate the detailed relationships between alterations in metabolite
266 levels and *H. pylori* infection experiments involving cultured cell lines and primary cells from an *H.*

267 *pylori*-infected host need to be carried out. In this study, the degree of changes was relatively small,
268 and this may be due to the diversity of the cells existed in the stomach tissues. The *in vitro*
269 experiments using involving cultured cell lines must lead to understandings of the clear changes of
270 metabolites. Moreover, comparative trials using a variety of *H. pylori* strains, for example, CagA-
271 negative *H. pylori* and *H. pylori* that expresses East-Asian-type CagA or Western-type CagA, are
272 also important.

273

274 **5. Conclusions**

275 In conclusion, our study showed that *H. pylori* infections cause various metabolite
276 alterations in host lesions, and different metabolite profiles were also observed between each phase
277 of the infection. Our study must be regarded as the first to have obtained novel findings regarding *H.*
278 *pylori* infections using the metabolome analysis.

279

280 **Funding**

281 This study was supported in part by a Grant-in-Aid for Scientific Research (B) (General) from the
282 Japan Society for the Promotion of Science (JSPS) [M.Y.]; a Grant-in-Aid for Scientific Research
283 (B) (Overseas Academic Research) from the JSPS [T.A.]; a Grant-in-Aid for Scientific Research (C)
284 (General) from the JSPS [S.N.]; and the AMED-CREST by the Japan Agency for Medical Research
285 and Development (AMED) [S.N., T.A. and M.Y.].

286

287 **Acknowledgements**

288 We are very grateful to Ms. Bregje Gräve (VU University Medical Center Amsterdam,
289 Amsterdam, Netherlands) for the research assistance she provided.

290

291 **Conflict of interest**

292 The authors declare that they have no conflict of interest.

293

294 **References**

- 295 [1] A. Morgner, E. Bayerdörffer, A. Neubauer, M. Stolte, Malignant tumors of the stomach. Gastric
296 mucosa-associated lymphoid tissue lymphoma and *Helicobacter pylori*, *Gastroenterol. Clin.*
297 *North. Am.* 3 (2000) 593-607.
298
- 299 [2] P.G. Isaacson, Recent developments in our understanding of gastric lymphomas, *Am. J. Surg.*
300 *Pathol.* 20(Suppl. 1) (1996) S1-7.
301
- 302 [3] S.J. Veldhuyzen van Zanten, P.M. Sherman, *Helicobacter pylori* infection as a cause of gastritis,
303 duodenal ulcer, gastric cancer and nonulcer dyspepsia: a systemic overview, *CMAJ.* 150 (1994)
304 177-185.
305
- 306 [4] IARC Working Group on the Evaluation of Carcinogenic Risks to Humans, Schistosomes, liver
307 flukes and *Helicobacter pylori*, *IARC Monogr. Eval Carcinog Risks Hum* 61 (1994) 1-241.
308
- 309 [5] J.G. Kusters, A.H.M. van Vliet, E.J. Kuipers, Pathogenesis of *Helicobacter pylori* infection, *Clin.*
310 *Microbiol. Rev.* 19 (2006) 449-490.
311
- 312 [6] M. Yoshida, N. Hatano, S. Nishiumi, Y. Irino, Y. Izumi, T. Takenawa, T. Azuma, Diagnosis of
313 gastroenterological diseases by metabolome analysis using gas chromatography-mass
314 spectrometry, *J. Gastroenterol.* 47 (2012) 9-20.
315
- 316 [7] S. Rochfort, Metabolomics reviewed: A new “Omics” platform technology for systems biology
317 and implications for natural products research, *J. Nat. Prod.* 68 (2005) 1813-1820.
318
- 319 [8] M. Suzuki, S. Nishiumi, T. Kobayashi, T. Azuma, M. Yoshida, LC-MS/MS-based metabolome
320 analysis detected changes in the metabolic profiles of small and large intestinal adenomatous
321 polyps in *ApcMin/+* mice, *Metabolomics.* 12 (2016) 1-9.

322

323 [9] A. Sakai, M. Suzuki, T. Kobayashi, S. Nishiumi, K. Yamanaka, Y. Hirata, T. Nakagawa, T.
324 Azuma, M. Yoshida, Pancreatic cancer screening using a multiplatform human serum
325 metabolomics system, *Biomark. Med.* 10 (2016) 577-586.

326

327 [10] Y. Terashima, S. Nishiumi, A. Minami, Y. Kawano, N. Hoshi, T. Azuma, M. Yoshida
328 Metabolomics-based search for therapeutic agents for non-alcoholic steatohepatitis, *Arch.*
329 *Biochem. Biophys.* 555-556 (2014) 55-65.

330

331 [11] X.X. Gao, H.M. Ge, W.F. Zheng, R.X. Tan, NMR-based metabonomics for detection of
332 *Helicobacter pylori* infection in gerbils: which is more descriptive, *Helicobacter.* 13 (2008) 103-
333 111.

334

335 [12] S. Backert, H. Gressmann, T. Kwok, U. Zimny-Arndt, W. König, P.R. Jungblut, T.F. Meyer,
336 Gene expression and protein profiling of AGS gastric epithelial cells upon infection with
337 *Helicobacter pylori*, *Proteomics.* 5 (2005) 3902-3918.

338

339 [13] V.J. Hofman, C. Moreilhon, P.D. Brest, S. Lassalle, K. Le Brigand, D. Sicard, J. Raymond, D.
340 Lamarque, X.A. Hébuterne, B. Mari, P.J. Barbry, P.M. Hofman, Gene expression profiling in
341 human gastric mucosa infected with *Helicobacter pylori*, *Mod. Pathol.* 20 (2007) 974-989.

342

343 [14] I. Nookaew, K. Thorell, K. Worah, S. Wang, M.L. Hibberd, H. Sjövall, S. Pettersson, J. Nielsen,
344 S.B. Lundin, Transcriptome signatures in *Helicobacter pylori*-infected mucosa identifies acidic
345 mammalian chitinase loss as a corpus atrophy marker, *BMC. Med. Genomics.* 6 (2013) 41.

346

347 [15] S.J. Hagen, M. Ohtani, J.R. Zhou, N.S. Taylor, B.H. Rickman, G.L. Blackburn, J.G. Fox,
348 Inflammation and foveolar hyperplasia are reduced by supplemental dietary glutamine during
349 *Helicobacter pylori* infection in mice, *J. Nutr.* 139 (2009) 912-918.

350

351 [16] K. Amagase, E. Nakamura, T. Endo, S. Hayashi, M. Hasumura, H. Uneyama, K. Torii, K.
352 Takeuchi, New frontiers in gut nutrient sensor research: prophylactic effect of glutamine against
353 Helicobacter pylori-induced gastric diseases in Mongolian gerbils, *J. Pharmacol. Sci.* 112 (2010)
354 25-32.

355

356 [17] E. De Bruyne, R. Ducatelle, D. Foss, M. Sanchez, M. Joosten, G. Zhang, A. Smet, F.
357 Pasmans, F. Haesebrouck, B. Flahou, Oral glutathione supplementation drastically reduces
358 Helicobacter-induced gastric pathologies, *Sci. Rep.* 6 (2016) 20169.

359

360 [18] A. Raitala, J. Karjalainen, S.S. Oja, T.U. Kosunen, M. Hurme, Helicobacter pylori-induced
361 indoleamine 2,3-dioxygenase activity in vivo is regulated by TGF β 1 and CTLA4 polymorphisms,
362 *Mol. Immunol.* 44 (2007) 1011-1014.

363

364 [19] T. Larussa, I. Leone, E. Suraci, I. Nazionale, T. Procopio, F. Conforti, L. Abenavoli, M.L.
365 Hribal, M. Imeneo, F. Luzza, Enhanced expression of indoleamine 2,3-dioxygenase in
366 Helicobacter pylori-infected human gastric mucosa modulates Th1/Th2 pathway and interleukin
367 17 production, *Helicobacter.* 20 (2015) 41-48.

368

369 [20] A.R. Hipkiss, Carnosine and its possible roles in nutrition and health, *Adv. Food. Nutr. Res.* 57
370 (2009) 87-154.

371

372 [21] K. Maemura, N. Shiraishi, K. Sakagami, K. Kawakami, T. Inoue, M. Murano, M. Watanabe,
373 Y. Otsuki, Proliferative effects of gamma-aminobutyric acid on the gastric cancer cell line are
374 associated with extracellular signal-regulated kinase 1/2 activation, *J. Gastroenterol. Hepatol.*
375 24 (2009) 688-696.

376

377 [22] H.F. Tsai, P.N. Hsu, Interplay between *Helicobacter pylori* and immune cells in immune
378 pathogenesis of gastric inflammation and mucosal pathology. *Cell. Mol. Immunol.* 7 (2010) 255-
379 259.
380
381 [23] G. Suarez, V.E. Reyes, E.J. Beswick, Immune response to *H. pylori*, *World. J. Gastroenterol.* 12
382 (2006) 5593-5598.
383
384

385 **Figure legends**

386 **Figure 1. Pathological appearance of stomach tissue from mice that had or had not been**
387 **infected with *Helicobacter pylori* SS1**

388 HE staining of stomach tissues from C57BL/6J mice that had or had not been infected with
389 *Helicobacter pylori* SS1 for 1 (1M), 3 (3M), or 6 (6M) months was performed (magnification: x40
390 or x 200). The panels show representative images from each group (N=4 each).

391

392 **Figure 2. The score plots in principal component analysis for the metabolite profile of stomach**
393 **tissue from mice that had or had not been infected with *Helicobacter pylori* SS1**

394 Principal component analysis was performed on the basis of the metabolite profile of
395 stomach tissue from mice that had or had not been infected with *Helicobacter pylori* SS1. The panels
396 show the results of the score plots consisting of Component 1, Component 2, and Component 3.
397 Open and closed symbols indicate the non infection and *H. pylori* SS1 infection groups, respectively.
398 Circle, triangle, and square symbols show 1 (1M), 3 (3M), and 6 (6M) month infection groups,
399 respectively.

Figure 1

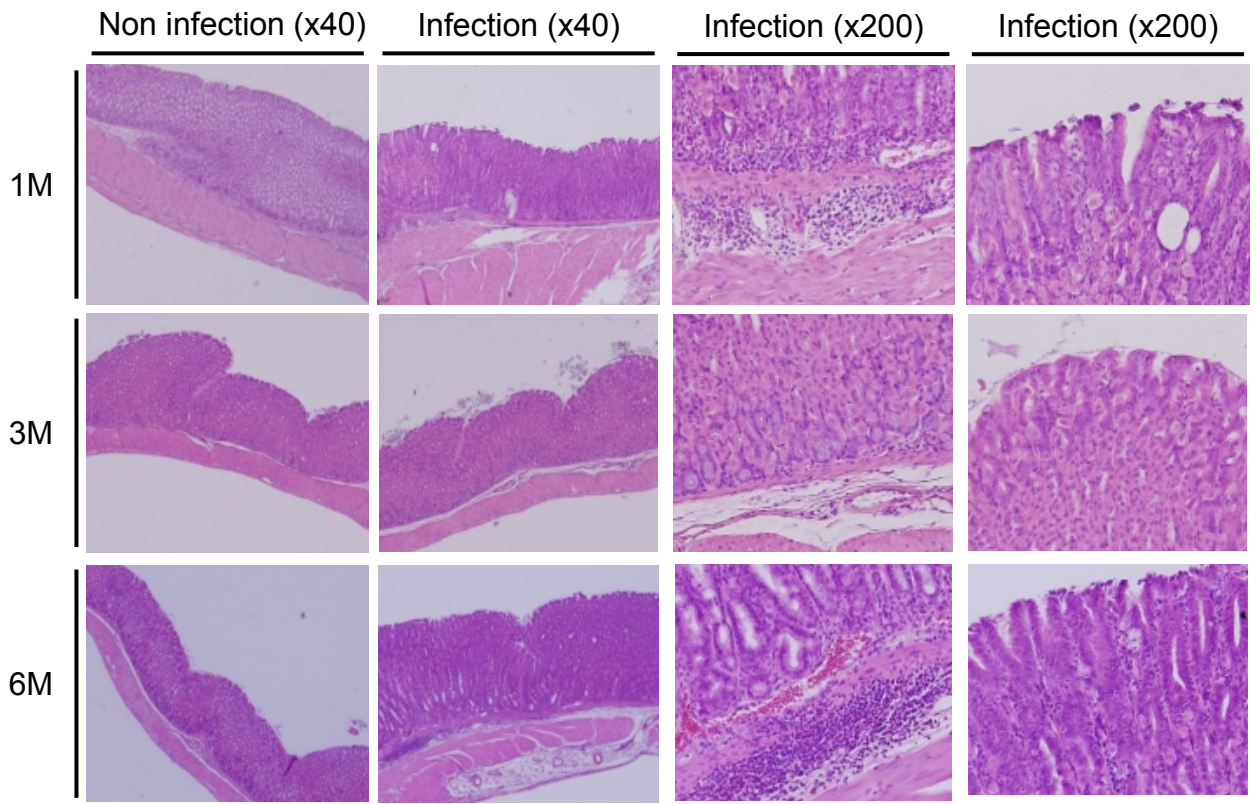


Figure 2

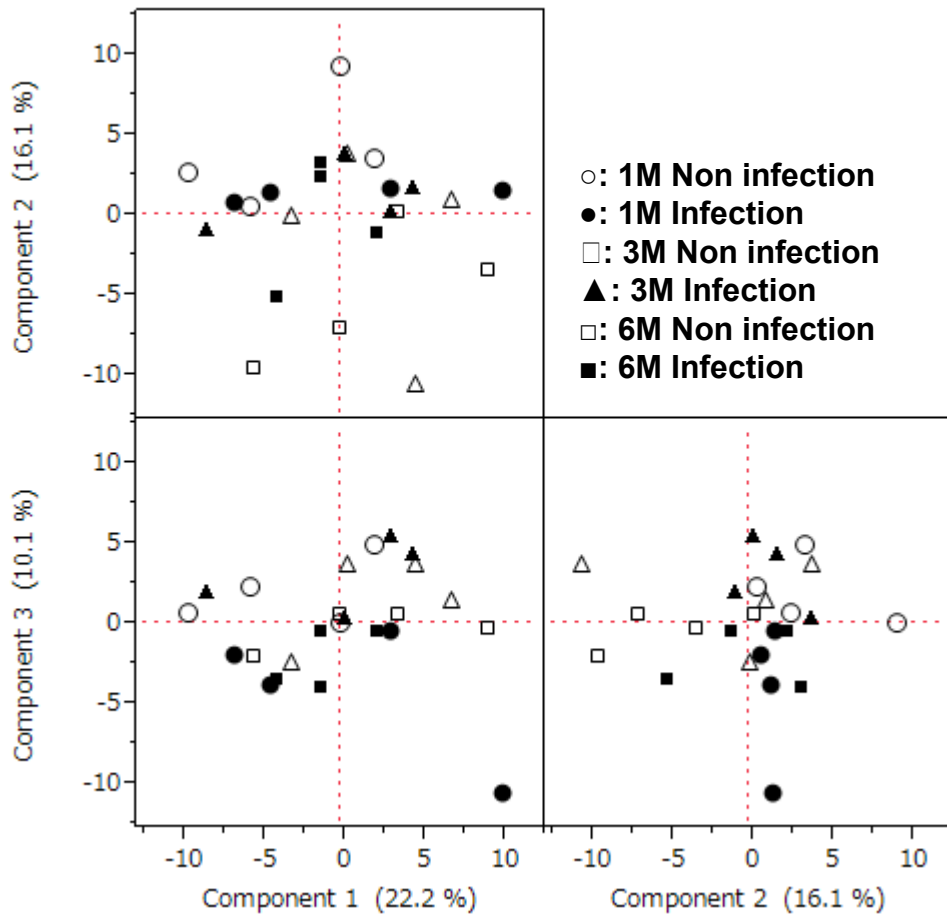


Table 1. Evaluation of metabolic pathways in the stomach tissues from the mice that had or had not been infected with *Helicobacter pylori* SS1

Pathway	Biochemical name	Fold induction values (infected/uninfected)			P-values (infected vs. uninfected)		
		1M	3M	6M	1M	3M	6M
Glycolysis	<u>Glu (glucose)</u>	1.26	0.89	0.76	0.22	0.80	0.073
	G6P (glucose-6-phosphate)	2.18	0.97	0.96	0.070	0.85	0.81
	F6P (fructose-6-phosphate)	2.11	0.87	0.99	0.11	0.38	0.96
	FBP (fructose-1,6-bisphosphate)	0.95	1.46	0.87	0.82	0.0015	0.31
	PEP (phosphoenol-pyruvate)	3.42	0.59	1.07	0.039	0.22	0.72
	2PG (2-phospho-glycerate)	1.68	0.82	0.96	0.25	0.29	0.91
	Glycerol-3P	1.35	0.93	1.02	0.12	0.73	0.89
TCA cycle	Pyruvate	1.66	1.08	1.11	0.0050	0.70	0.42
	Lactate	1.20	0.96	1.04	0.083	0.42	0.68
	Oxaloacetate	1.05	1.03	1.31	0.81	0.74	0.22
	Citrate	1.02	0.94	1.16	0.95	0.76	0.55
	cis-aconitate	1.09	0.97	1.08	0.40	0.63	0.46
	Isocitrate	1.07	1.01	1.07	0.76	0.94	0.74
	2-ketoglutarate	1.61	1.10	0.62	0.075	0.69	0.053
	Succinate	1.66	0.92	0.70	0.10	0.60	0.13
	Fumarate	0.99	0.90	1.19	0.96	0.17	0.0072
	Malate	1.60	1.35	0.77	0.18	0.17	0.28
Choline pathway	Choline	1.52	0.90	0.87	0.070	0.51	0.048
	Phosphocholine	2.95	0.91	1.30	0.013	0.74	0.28
Purine pathway	<u>Hypoxanthine</u>	0.74	0.93	1.02	0.0055	0.59	0.87

	<u>Adenine</u>	1.18	0.89	0.70	0.49	0.48	0.043
	<u>Xanthine</u>	0.42	1.50	1.81	0.20	0.44	0.45
Pyrimidine pathway	Cytidine	1.45	0.90	0.85	0.24	0.52	0.027
	Cytosine + Histamine	1.03	1.15	0.53	0.87	0.70	0.30
	β -alanine	1.15	0.93	0.92	0.62	0.72	0.66
	Uridine	1.42	0.84	0.75	0.43	0.39	0.028
	<u>Uracil</u>	0.77	0.87	1.38	0.12	0.54	0.036
	Aspartate	1.18	0.94	0.77	0.19	0.80	0.16
Urea cycle	Aspartate	1.18	0.94	0.77	0.19	0.80	0.16
	Fumarate	0.99	0.90	1.19	0.96	0.17	0.0072
	Oxaloacetate	1.05	1.03	1.31	0.81	0.74	0.22
	Malate	1.60	1.35	0.77	0.18	0.17	0.28
	Arginine	0.89	0.86	0.78	0.43	0.35	0.018
	Ornithine	1.01	1.15	0.73	0.95	0.59	0.040
	Citrulline	0.93	0.80	0.94	0.79	0.14	0.64
	<u>Urea</u>	1.16	0.66	1.04	0.51	0.045	0.91
	Glutamate	1.24	0.83	0.84	0.099	0.22	0.30
	Creatine	1.39	0.92	0.71	0.013	0.55	0.0060
	Creatinine	1.00	1.06	0.87	0.96	0.59	0.00091
	<u>GABA (γ-aminobutyrate)</u>	0.94	0.72	0.44	0.54	0.41	0.038
	Succinate	1.66	0.92	0.70	0.10	0.60	0.13
	Orotate	1.11	0.76	1.02	0.55	0.011	0.85
Glutathione cycle	Glycine	1.14	0.87	0.81	0.41	0.42	0.057
	Cysteine	0.75	1.01	1.15	0.061	0.93	0.042
	Glutamate	1.24	0.83	0.84	0.099	0.22	0.30

	Cystathionine	1.00	0.61	1.30	0.98	0.054	0.070
	Serine	0.96	1.09	0.88	0.52	0.36	0.17
	SAH (S-adenosyl-L-homocysteine)	1.92	0.75	0.85	0.0023	0.19	0.36
	Methionine	0.88	0.99	0.79	0.41	0.97	0.086
Amino acid metabolism	Glycine	1.14	0.87	0.81	0.41	0.42	0.057
	Alanine + Sarcosine	1.31	0.94	0.92	0.30	0.75	0.65
	Arginine	0.89	0.86	0.78	0.43	0.35	0.018
	Aspartate	1.18	0.94	0.77	0.19	0.80	0.16
	Asparagine	0.94	0.98	0.73	0.58	0.88	0.0047
	Cysteine	0.75	1.01	1.15	0.061	0.93	0.042
	Lysine	1.05	0.98	0.90	0.70	0.91	0.54
	Glutamine	1.29	0.83	0.83	0.058	0.21	0.22
	Glutamate	1.24	0.83	0.84	0.099	0.22	0.30
	Histidine	1.11	0.86	0.69	0.31	0.44	0.0037
	Isoleucine	0.92	0.96	0.97	0.51	0.65	0.89
	Leucine	1.01	0.96	0.96	0.96	0.72	0.84
	Methionine	0.88	0.99	0.79	0.41	0.97	0.086
	Phenylalanine	1.05	0.81	0.78	0.65	0.33	0.044
	Proline	1.00	0.98	0.73	0.99	0.92	0.086
	Serine	0.96	1.09	0.88	0.52	0.36	0.17
	Threonine	0.82	1.05	1.11	0.33	0.80	0.59
	Tryptophan	0.87	1.07	0.90	0.32	0.56	0.56
	Kynurenine	1.06	1.80	1.46	0.80	0.033	0.19
	Tyrosine	0.93	1.02	0.70	0.65	0.95	0.011
	Valine	0.88	0.95	0.94	0.24	0.70	0.64
	β -alanine	1.15	0.93	0.92	0.62	0.72	0.66
	4-hydroxy-L-proline	1.01	0.86	0.97	0.97	0.37	0.84

<u>GABA (γ-aminobutyrate)</u>	0.94	0.72	0.44	0.54	0.41	0.038
Glycolate	1.00	1.09	1.50	0.98	0.59	0.15

Fold induction values (infected/uninfected) and p-values (obtained from comparisons between the infected and uninfected mice) for the metabolites involved in the glycolytic pathway; TCA cycle; choline pathway; urea cycle; glutathione cycle; purine pathway; pyrimidine pathway; or amino acid metabolism, including the glutamine pathway and tryptophan cycle, are shown. The infected mice were infected with *Helicobacter pylori* SS1 for 1 (1M), 3 (3M), or 6 (6M) months. The number of 1, 3 or 6 month infection groups and the corresponding non-infection groups was N=4 each. P-values of less than 0.05 and the corresponding fold inductions are indicated by bold letters. The underlined metabolites were analyzed using GC/MS analysis, and the other metabolites were analyzed using LC/MS analysis.

Table 2. Evaluation of metabolite levels in stomach tissue from mice that had or had not been infected with *Helicobacter pylori* SS1

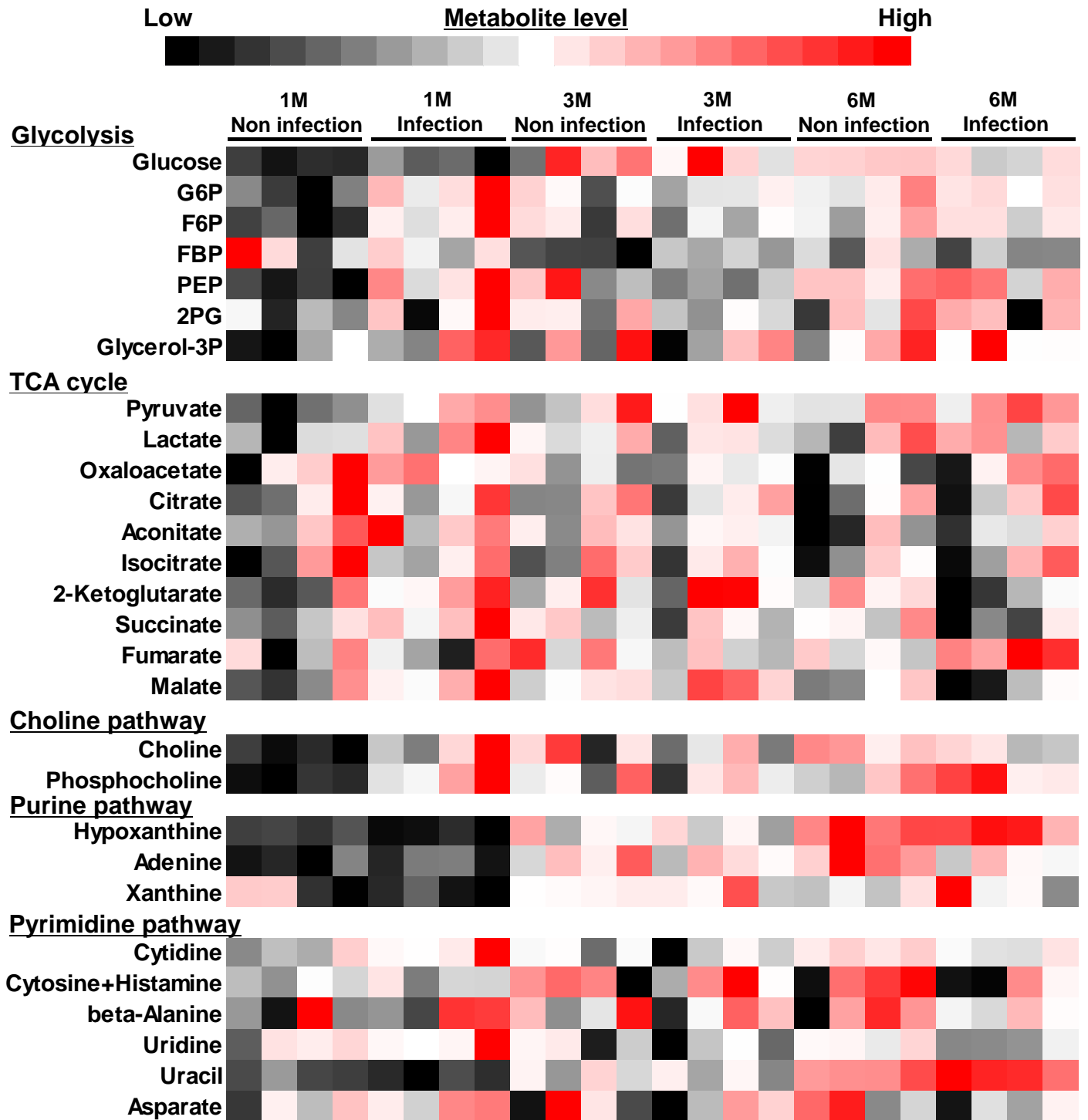
Biochemical name	Fold induction values (infected/uninfected)			P-values (infected vs. uninfected)		
	1M	3M	6M	1M	3M	6M
3-hydroxy-butyrate	0.93	1.06	1.57	0.58	0.59	0.042
3-hydroxy-2-methyl-butanoate (2-methyl-3-hydroxybutyrate)	1.21	0.93	0.94	0.39	0.72	0.76
Benzoate	0.88	0.92	1.07	0.40	0.71	0.70
Mesaconate	1.02	0.98	1.03	0.77	0.68	0.61
Ethyl-malonate	1.05	1.13	1.25	0.83	0.26	0.38
o-toluate	1.22	1.01	0.97	0.63	0.99	0.90
3-methyl-glutarate	0.88	0.91	0.77	0.41	0.50	0.098
2-hydroxy-phenylacetate	0.78	0.93	1.02	0.17	0.66	0.82
3-hydroxy-3-methyl-glutarate	0.80	0.77	0.86	0.48	0.34	0.66
Tricarballylate	1.22	1.04	1.01	0.59	0.90	0.98
Azelate	0.86	0.82	0.91	0.45	0.47	0.76
Glucuronate	1.16	1.02	1.04	0.48	0.94	0.80
N-acetylneuraminate	1.17	1.07	0.85	0.35	0.72	0.46
2-hydroxy-isobutyrate	1.04	1.16	1.01	0.59	0.10	0.87
3-hydroxy-3-methyl-butanoate (3-hydroxyisovalerate)	0.94	1.22	1.12	0.69	0.28	0.45
4-methyl-2-oxovalerate	1.03	0.85	1.00	0.87	0.25	0.98
2-hydroxy-isocaproate	0.64	1.38	1.35	0.21	0.29	0.22
p-hydroxybenzoate	0.67	0.85	1.04	0.081	0.45	0.90
2-ethylhexanoate	0.97	1.10	1.02	0.78	0.28	0.76
2-hydroxy-glutarate	1.07	0.75	0.87	0.62	0.030	0.51
Phthalate (benzene-1,2-dicarboxylate)	0.84	1.08	1.05	0.070	0.27	0.60
4-hydroxy-phenyl-lactate	1.04	1.04	0.72	0.91	0.88	0.25
Phosphorate	1.11	0.88	0.98	0.32	0.19	0.73
Levulinate	1.13	0.98	0.95	0.27	0.87	0.83

Citraconate	0.99	1.05	0.97	0.91	0.35	0.69
Octanoate (caprylate)	0.94	1.03	1.04	0.59	0.50	0.36
2-oxoadipate	1.05	1.25	1.36	0.79	0.43	0.22
β -phenyl-lactate	0.92	0.93	0.99	0.85	0.79	0.94
3-hydroxy-propionate	1.00	1.03	0.84	0.98	0.79	0.37
3-hydroxy-isobutyrate	0.84	1.08	1.21	0.42	0.66	0.44
Glycerate	1.37	1.01	1.02	0.029	0.89	0.85
2-hydroxy-3-methyl-butyrate (2-hydroxyisovalerate)	0.88	1.09	1.42	0.37	0.57	0.040
Glutaconate	0.92	0.98	0.99	0.33	0.82	0.89
Glutarate	1.31	1.13	0.84	0.52	0.49	0.61
Threonate	0.99	1.14	0.99	0.94	0.17	0.86
Pimelate	0.96	0.97	1.18	0.70	0.62	0.38
Quinate	1.04	0.94	0.85	0.66	0.52	0.29
Gluconate	1.14	0.97	1.44	0.45	0.90	0.12
Saccharate	1.75	0.70	0.76	0.58	0.38	0.44
Betaine	1.48	0.91	0.84	0.14	0.81	0.50
Carnitine	1.20	1.14	1.02	0.18	0.12	0.85
Carnosine	1.22	0.78	0.78	0.37	0.24	0.025
Homoserine	0.82	1.07	1.07	0.34	0.74	0.72
Norvaline	0.88	0.98	0.91	0.30	0.84	0.49
Dimethylglycine	1.42	1.04	1.58	0.29	0.90	0.21
Homocysteine	0.82	1.12	1.13	0.14	0.38	0.29
Cystine	0.75	1.20	1.24	0.18	0.34	0.41
N-acetylglycine	0.79	1.14	1.63	0.25	0.39	0.010
N-isovaleroylglycine	1.48	1.08	0.88	0.15	0.81	0.76
Pyroglutamate	1.08	0.95	0.79	0.43	0.71	0.014
N-acetyl-L-aspartate	1.62	0.77	0.77	0.094	0.22	0.17
N-acetyl-L-tyrosine	0.76	1.13	0.47	0.28	0.79	0.059

Serotonin	4.67	0.20	0.63	0.000030	0.33	0.56
2'-deoxycytidine	1.03	0.94	1.14	0.73	0.66	0.22
Taurine	1.17	0.80	1.09	0.32	0.081	0.38
N-acetyl-DL-alanine	0.93	1.37	0.85	0.69	0.24	0.38
Acetyl-L-glutamine	1.12	0.88	0.94	0.57	0.34	0.50
2-aminobutyrate	1.49	0.90	1.55	0.27	0.71	0.27
Urate	1.62	0.65	0.74	0.064	0.15	0.039
N-acetylneuraminate	1.11	0.88	1.06	0.36	0.61	0.38

Fold induction values (infected/uninfected) and p-values for the metabolites that were not related to the glycolytic pathway, TCA cycle, choline pathway, urea cycle, glutathione cycle, purine pathway, pyrimidine pathway, or amino acid metabolism are shown. The infected mice were infected with *Helicobacter pylori* SS1 for 1 (1M), 3 (3M), or 6 (6M) months. The number of 1, 3 or 6 month infection groups and the corresponding non-infection groups was N=4 each. P-values of less than 0.05 and the corresponding fold induction values are indicated by bold letters.

Supplemental Figure 1



Supplemental Figure 1. Heat-map representation for each metabolite pathway

Regarding each metabolite pathway shown in Table 1, the relative values of the metabolites were represented by colors in the heat map. In the heat-map representation, 1M, 3M, and 6M indicate 1 month, 3 month, and 6 month, respectively.

Highlights

We performed metabolome analysis of the stomach tissue of mice that had been infected with H. pylori SS1 for 1, 3, or 6 months.

We evaluated the H. pylori infection-induced modulation of various metabolic pathways via metabolite profiling.

H. pylori infection caused various metabolite alterations at lesional sites.